

Article

Transient Stability-Based Fast Power System Contingency Screening and Ranking

Teshome Lindi Kumissa ^{1,*}  and Fekadu Shewarega ²

¹ School of Electrical and Computer Engineering (SECE), Hawassa University Institute of Technology, Hawassa D-45117, Ethiopia

² Institutes of Electrical Power Systems, University of Duisburg-Essen, D-45117 Duisburg, Germany; fekadu.shewarega@uni-due.de

* Correspondence: teshomel@hu.edu.et

Abstract: Today's power systems are operated closer to their stability limits due to the continuously growing load demands, interface to open markets, and integration of more renewable energies. In order to provide operators with clear insight on the current system situation, near real-time power systems dynamic security assessment tools are required. One of the core elements of near real-time dynamic security assessment tools is contingency screening and ranking. Most of the commercially available tools screen and rank contingencies by using the traditional numerical integration or Transient Energy Functions (TEFs) or hybrid methods. The traditional numerical integration method is accurate but computationally intensive and has a slow assessment speed which makes it difficult to identify any insecure contingency before it happens. Despite the TEF method of transient stability analysis being relatively fast, it develops less accurate results due to models simplification and assumptions. This paper introduces transient stability based on fast and robust contingency screening and ranking using an Adaptive step-size Differential Transformation (AsDTM) method. Based on the most current snapshot from Supervisory Control and Data Accusation (SCADA) data, the proposed method triggers AsDTM-based transient stability simulation for each credible contingency and evaluates Transient Stability Indices (TSI) as the normalized weighted sum of squares of errors derived from state variables and complex bus voltages at every simulation time step. Finally, contingencies are ranked based on these TSI and the worst contingency is identified for the next detail assessment. The method is tested on IEEE 9 bus and 39 bus test systems. Test results reveal that the proposed method is faster, robust, and can be used in near real-time dynamic security assessment sessions.

Keywords: transient stability indices (TSI); dynamic security assessment (DSA); transient stability simulation; contingency screening



Citation: Kumissa, T.L.; Shewarega, F. Transient Stability-Based Fast Power System Contingency Screening and Ranking. *Electricity* **2024**, *5*, 947–971. <https://doi.org/10.3390/electricity5040048>

Academic Editor: Murilo E.C. Bento

Received: 19 September 2024

Revised: 11 November 2024

Accepted: 19 November 2024

Published: 25 November 2024



Copyright: © 2024 by the authors. Licensee MDPI, Basel, Switzerland. This article is an open access article distributed under the terms and conditions of the Creative Commons Attribution (CC BY) license (<https://creativecommons.org/licenses/by/4.0/>).

1. Introduction

A reliable electricity supply is foundational to all economic and societal activities in modern societies. Ensuring the secure operation of the system during widely varying loading scenarios or following possible unforeseen events represents an immense challenge to the system operator. To assess the security risk correctly and to initiate any necessary corrective measures, the operator needs to have situational awareness at all times. Most of the recent methods of stability assessment are based on extensive off-line computations and, consequently, may no longer be sufficient; hence, a near real-time DSA is significantly demanding [1]. The near real-time application of a DSA to a realistic network needs sufficient methods to screen and rank large number of contingencies to be investigated by DSA tools.

The goal of contingency screening and ranking is to shortlist critical contingencies for deeper evaluation of the power system. Since, in practice not every contingency will bring an instability problem to the power system, conformation of a critical contingencies list is created according to the comparisons of the performances of the power system [2,3]. The performances of the power system after being subject to each contingency are evaluated with respect to the capacities of the equipment, operating constraints, etc. During contingency screening, contingencies with a small influence on system operation are removed. Their exclusion from credible contingencies lists results in a significant reduction in information for near real-time operation, i.e., only a few potentially severe contingencies are considered to undergo detailed evaluation. Several broad approaches to contingency screening and ranking methods have been proposed [4].

The authors of [5,6] proposed some indices for contingency screening and ranking. However, they often require numerical integration for a significant interval after the fault clearance. Ref. [6] proposes heuristic individual and global transient instabilities indices based on combined numerical integration and direct methods (hybrid method) for contingency screening in an online DSA session. The method proposed by [7] is based on simplified modeling with assumptions which can result in substantial simulation errors. Transient stability simulation-based indices for contingency screening and ranking are proposed by [8], which solves both differential and algebraic equations of a power system numerically by a MATLAB ODE solver. Approaches, such as a numerical integration, direct (energy function methods), and combination of both methods, are explored by [9–11]. The conventional numerical integration-based methods are accurate but require intensive computations; but direct methods are the reverse.

In [12], various severity indices for dynamic security analysis and the ranking of contingencies are proposed. For the purpose of measuring the severity of a contingency, the authors propose several indices, which are based on coherency, transient energy conversion, and dot products of certain system states. Finally, the authors propose a composite index, which assigns different weights to the prior defined indexes and sums up their contributions. In this approach, a detailed time-domain simulation is carried out until 500 ms after fault clearance. Then, the indices are computed to determine stability and to rank the respective contingencies. However, the majority of the indexes do not obviously divide the contingencies into unstable and stable scenarios while tested being used with a particular test case. Power system contingency screening and a ranking method based on the TEF method was proposed by [13]. The method utilizes the transient energy function and aims at filtering out the non-severe disturbances. The TEF method has received a lot of attention and assessment methods based on it were continuously advanced.

Hybrid methods, like SIME [10], improve the transient stability simulation speed. The method consists of two blocks. The first block filters stable contingencies and the second block ranks and assesses the remaining possible harmful contingencies based on their estimated critical clearing times (CCTs). This requires running time-domain simulations twice per contingency. In [14], a fast power system contingency screening technique based on SIME was presented. A new index was introduced for grouping generators as well as a contingency classification based on the power angle shape of the one-machine infinite bus (OMIB) equivalent. For this purpose, the method requires running time-domain simulations one to three times per contingency with varying fault clearing times. Alternatively, contingency screening methods, which are executed periodically, and the deployment of wide-area measurement systems in power systems enabled transient stability prediction utilizing real-time synchronized phasor measurements.

A contingency screening method utilizing the extended equal area criterion (EEAC) as described in [15] was presented in [16]. The EEAC is a further development of the equal area criterion (EAC) to allow an application of the criterion to multi-machine systems. The authors derived a set of rules to effectively filter out the stable cases from a set of credible

contingencies. In order to identify and filter stable cases, just after fault clearance the stability margins determined from the static EEAC (SEEAC) and dynamic EEAC (DEEAC, as described in [17,18]) are computed. Then, the aforementioned rules are employed to identify if a case is stable and should be filtered out.

In [19], the authors propose a method to predict transient rotor swings using a fuzzy hyper-rectangular composite neural network and post-contingency phasor measurements to determine stability. Recently, a method for transient stability prediction and mitigation has been proposed by [20]. The method uses real-time measurements provided from phasor measurement units (PMUs) and an artificial neural network (ANN) to detect stability or instability of the power system. If instability is detected, a remedial action scheme is activated. This method improves the computation speed, but the detail system model is not supported. However, these methods require training on a forecast database and provide a certain degree of generalization that may not always be capable of correctly determining security and stability [4].

The review of works to advance power system contingency screening and ranking methods presented above can be summarized and grouped into four broad methods as a traditional numerical integration method of TDS, direct (TEF) methods, a hybrid of TDS and TEF methods, and automating learning methods (such as methods based on ANN). Approaches such as a power system TDS based on numerical integrations provide accurate assessment results but are too slow due to their intensive computation requirement. Transient energy function and hybrid methods proposed by different authors may provide quantitative measures which indicate the degree of system stability based on the energy margin or stability indices but require model simplification and assumptions. Since the generation and consumption pattern in the system become less predictable and dependent on forecasting accuracies, methods based on off-line databases, such as ANN, a decision tree, pattern recognition methods, etc, are going to be challenged by the vast amount of possible operating conditions [4]. It is likely that these very unpredictable situations are not part of the database and may even deviate significantly from the scenarios in the database.

To mitigate these problems, some advanced time-domain simulations have been proposed in different literatures. The analytical method of transient stability assessment recently proposed in [21] is a non-iterative method of solving complex power system differential algebraic model equations by using a differential transformation method. In this approach, a fully analytical solution method is used, no network simplifications are made, and loads are not assumed as a constant impedance load. However, the differential transformation method generates a series solution, actually a truncated series solution which does not exhibit the real behaviors of the problem but gives a good approximation to the true solution in a very small region. A multi-step differential transformation approach is required to extend the region of solution and improve the simulation speed and accuracy of the resulting solution [22,23]; in some cases, a very small sub-division of interval is required with this method, which actually results in a greater computational burden and more time.

To overcome the drawback of this differential transformation method, an adaptive step-size differential transformation method (AsDTM) is proposed by [24]. The proposed method introduces a novel step-size control algorithm based on local convergence error results at the end of each simulation time step. The method adaptively varies the step-size of classical DTM- based simulation method. The step size is varied based on the local truncation error control algorithm. The automatic controls of the step-size length are performed based on the principles: (1) reduce the time step length when the error is above the tolerable error limit, to improve the accuracy of the simulation, and (2) increase the time step length when the error is below the tolerable error limit, to avoid an unnecessary computational burden and improve the overall efficiency.

This paper introduces a fast and robust power system contingency screening and ranking method, whose performance is suitable for a near real-time application and could be a part of a DSA toolbox. Power system transient stability analysis based on an AsDTM is used in this paper. TS indices are evaluated from the analysis results as normalized weighted sums of squares of error at every simulation time step for both state variables and complex bus voltages. This work has at least four major contributions: (1) It is relatively robust and accurate, because it is flexible in handling power systems with any model detail and complexity without limitations, for instance, complex high-order models of AVRs, turbine, governors, boilers, SVCs, and other items of plant can be used; (2) it improves simulation speed and accuracy based on the control of the local convergence error at each time step; (3) the local solution error is estimated from only the last coefficient terms of the state and algebraic variables without any further calculations as in the variable step-size algorithm using traditional numerical integration methods; and (4) the solution obtained for the current simulation time step can be used during the next simulation time step without any limitations, such that the number of steps required to complete the transient stability simulation process reduces. Therefore, using the AsDTM method reduces the time spent in filtering out the potentially severe contingencies and reduces the update time of the DSA system. These enable the proposed method to be applied in a near real-time DSA session. Using the proposed comprehensive methodology, case studies are performed on IEEE 9 bus and New England IEEE 39 bus test systems and validated.

The paper is organized as follows. Section II describes the proposed method; Section III presents test results of the proposed approach on IEEE 9 bus and New England IEEE 39 bus test systems, and Section IV presents conclusions and future work

2. The Proposed Contingency Screening and Ranking Method

In a near real-time DSA tool, power system contingency screening and ranking is expected to be executed periodically several times per day. In order that a large number of contingencies can be processed by a near real-time DSA system, it is necessary to include some form of contingency screening to filter out those contingencies which lead to little or no degradation of the system security [1]. This will reduce the time spent in filtering out the potentially severe contingencies and reduce the update time of the DSA system. At the same time, it is very important that all the contingencies that will lead to stability problems are identified, i.e., the screening process is accurate.

In this paper, contingency screening and ranking using an AsDTM-based power system transient stability analysis is proposed. The proposed method starts whenever the system operators require analyzing the impact of some set of selected contingencies for the purpose of a near real-time operation using the most current system operating state data as the basis. At each time step of the transient stability analysis for every credible contingency, the TSI (AI and SI) is evaluated as a weighted sum of squares of errors derived from state variables and complex bus voltages at every time step, during the process of transient stability simulations for each credible contingency. These indices are related by normalizing them with the largest of all and ranked. Finally, the worst contingency is identified for the next detail assessment. The TS indices evaluated based on the machine's state variables are represented as the machine's state variables indices (SI) and those evaluated based on the machine's bus complex bus voltages are represented as algebraic indices (AI).

Note that the method does not aim at predicting the transient response of the system after the occurrence of a fault; instead, the method carries out a contingency screening and ranking to ensure that the system is transiently stable with respect to a given set of credible contingencies. Figure 1 shows the flowchart diagram of the proposed contingency screening and ranking method assumed to be integrated into the near real-time DSA session. In the following subsections, each part of the proposed algorithm will be described in more detail.

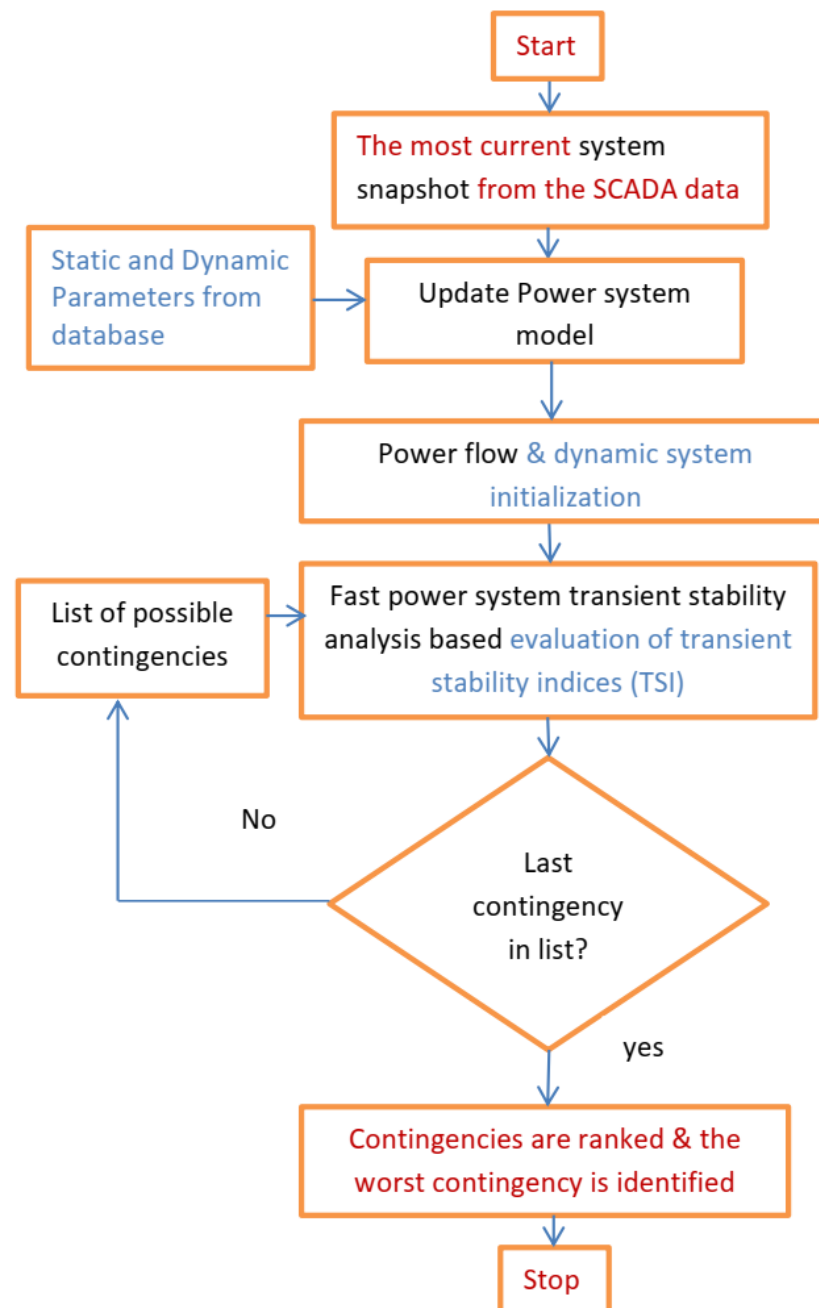


Figure 1. Flowchart diagram of the proposed power system contingency screening and ranking method integrated into a framework for near real-time application.

2.1. The Most Current System Snapshot from the SCADA Data

The most current system snapshots consisting of complex power flows through transmission lines, complex power injections (generation or demand at buses), and bus voltage magnitudes are read from Supervisory Control and Data Acquisition (SCADA) data. These data are used to represent the system's pre-fault condition so as to initialize the transient stability simulations.

2.2. Static and Dynamic Parameters from the Database

The static and dynamic data contain a system model parameter for all components in the monitored power system. The provided parameters are assumed to be enough to represent the power system components with proper detail to enable an accurate simulation

of the transient response. In this paper, the synchronous generator's rotor dynamics are represented by a fourth-order model.

2.3. Update Power System Models

The obtained most current system snapshot and the model database, which provide the required dynamic and static data and parameters of each component, are utilized to set up the power system models representing the current system state including the network admittance matrix Y .

2.4. Perform Power Flow, Initialize Dynamic System, and Prepare List of Credible Contingencies

Using the updated power system model, a power flow analysis is performed to represent the system's pre-fault steady state conditions and hence initialize the dynamic system for the next power system transient stability analysis-based evaluation of the TSI function based on the flowchart given by Figure 2. A list of credible contingencies is also generated for the system under consideration here.

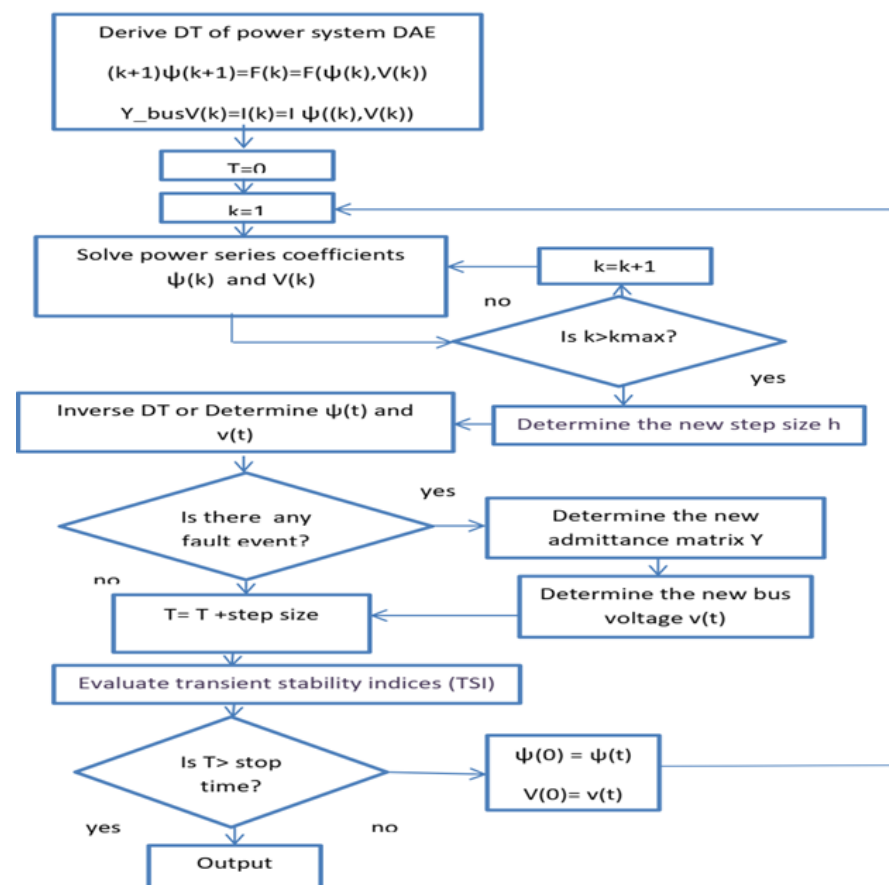


Figure 2. Flowchart of the algorithm for fast transient stability-based TSI evaluation.

2.5. Fast Power System Transient Stability Analysis-Based TSI Evaluations

2.5.1. Differential Transformation Method (DTM)

The theory of the differential transformation method is originally established in [25] to derive approximate solutions of nonlinear differential equations and is defined as below. Consider a function $\psi(t)$ of a real continuous variable t . The differential transformation of $\psi(t)$ is defined by Equation (1), and the inverse DT of $\psi(k)$ is defined by Equation (2), where k is the order transformation.

$$\psi(k) = \frac{1}{k!} \left[\frac{d^k \psi(t)}{dt^k} \right]_{(t=0)} \quad (1)$$

$$\psi(t) = \sum_{k=1}^{\infty} \psi(k)t^k \tag{2}$$

Next, it is developed by researchers in the fields of mathematics and physics to obtain semi-analytical solutions of various nonlinear dynamic systems. In [20,21], this method was examined for real-life complex network systems such as power systems modeled by high-order nonlinear differential equations. DTM provides a set of transform rules. Some of these transform rules are listed below. If we let $x(t)$, $y(t)$ and $z(t)$ be the original functions and $X(k)$, $Y(k)$, and $Z(k)$ their DTs, respectively, the following propositions hold, where c is a constant matrix and n is a nonnegative integer [26]:

- (a) $X(0) = x(0)$.
- (b) $y(t) = cx(t) \rightarrow Y(k) = cX(k)$.
- (c) $z(t) = x(t) \pm y(t) \rightarrow Z(k) = X(k) \pm Y(k)$.
- (d) $z(t) = x(t)y(t) \rightarrow Z(k) = \sum_{m=0}^k X(m)Y(k-m)$
- (e) $Z(t) = \frac{y(t)}{h(t)}$ its sDT = $\frac{1}{H(0)} \left(Y(k) - \sum_{m=0}^{k-1} H(k-m)Z(m) \right)$
- (f) $x(t)^T = X(k)^T$
- (g) $dx/dt = (k+1)X(k+1)$ and if DT of $\sin \delta = \varphi(k)$ and DT of $\cos \delta = \alpha(k)$ then
- (h) $\varphi(k) = \left(\sum_{m=0}^{k-1} \frac{k-m}{k} \alpha(m) \delta(k-m) \right)$
- (i) $\alpha(k) = \left(-\sum_{m=0}^{k-1} \frac{k-m}{k} \varphi(m) \delta(k-m) \right)$

The use of DTM as an explicit solver of power-system complex differential algebraic equations (DAEs) in power-system dynamic simulation presented by [21,24] introduces a significant advancement in power system dynamic simulation. It is proven that the performance efficiency of a DTM is much better than that of the traditional numerical integration methods, because when using the DTM method, the iteration to solve algebraic equations after each integration step is eliminated and has a higher radius of convergence. The procedures to solve multi-machine power system DAE models using the DTM method is as follows [21]: (1) transform power system DAE equations, (2) calculate the coefficients of state and algebraic variables, and (3) perform an inverse transformation to determine state and algebraic variables as a function of time.

Implementations of the DTM-based solution method is illustrated using an initial value problem as presented below.

Consider the following initial value problem: Equation (3), where $C \in R^m$ and $F : R^m \rightarrow R^m$:

$$\begin{aligned} \frac{d\psi}{dt} &= F(\psi(t), t), \quad 0 \leq t \leq T, \\ \psi(0) &= c \end{aligned} \tag{3}$$

where $\psi = (\psi_1, \psi_2, \dots, \psi_n)$ and the interval $[0, T]$ is partitioned into N subdomains with grid points expressed as $t_0, t_1, \dots, t_{j-1}, t_j = T$, such that $t_{j+1} = t_j + h$. Using the DTM solution approach, the first step is to determine the DTs of Equation (3), which is given as Equation (4) below, where K is the order of DT and m is the number of variables:

$$\begin{aligned} \psi_{m,n}(k) &= \frac{1}{k} [F(k, t_n)] \\ k &= 0, 1, 2, \dots, K \ \& \ n = 0, 1, 2, \dots, N - 1 \end{aligned} \tag{4}$$

By eliminating $1/k$ from the right side of Equation (4), we can rewrite it as Equation (5), where ψ_{mn} and F are the transformed vector valued functions:

$$\psi_{m,n}(k) = F(\psi_{mn}(k-1), t_n) \tag{5}$$

As we can see from Equation (5) above, the coefficient terms $\psi_{m,n}(k)$ can be explicitly determined from the lower-order coefficient terms recursively based on Figure 3.

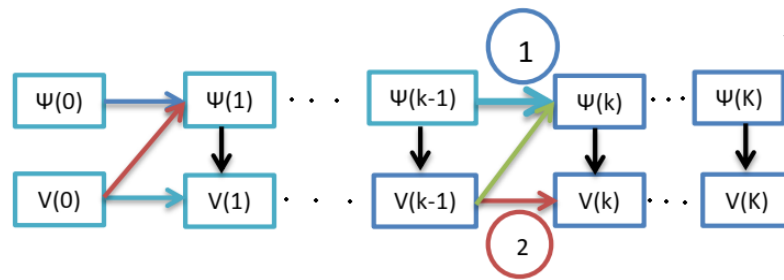


Figure 3. Recursive process to solve power series coefficients source [21].

After all the coefficient terms from $k = 0$ up to $k = K$ are known, the exact solution of Equation (3) at a point $t = t_{n+1} = t_n + h$ can be written in the form of a Taylor expansion, considering m to be the number of variables, as in Equation (6), where h represents the step size:

$$\psi_m(t_{n+1}) = \sum_{k=0}^{\infty} \psi_{mn}(k)h^k = \sum_{k=0}^K \psi_{mn}(k)h^k + h\xi_n \tag{6}$$

where ξ_n is a local truncation error and $n = 0, 1, 2, \dots, N - 1$. The local truncation error can be expressed in the form of a residual formula of Taylor series, considering m to be the number of vectors of variable ψ_n , and is expressed as Equation (7):

$$\begin{aligned} \xi_n &= \psi_{mn}(k)h^k = h^k F(\psi(k-1), t_c) \\ &= h^k \left[\frac{d^k f(\psi_m(t), t)}{dt^k} \right]_{t=t_c} \tag{7} \\ t_c &\in (t_n, t_{n+1}) \end{aligned}$$

This shows that the DTM method approximates locally to the exact solution with the order k .

AsDTM-based analysis in which the step size h is varied based on imposing the maximum of absolute values of the last coefficient terms to be lower than the admissible local error [24] is applied in this paper. This can be obtained by replacing ξ_n in Equation (7) by the admissible local error σ . Therefore, the new step size is calculated from Equation (8), where σ is the admissible local truncation (solution) error:

$$\begin{aligned} E &= \max |(\psi_{mn}(k))| \\ \sigma &= Eh^k \rightarrow h_{new} = \left(\frac{\sigma}{E} \right)^{\frac{1}{k}} \leq h_{max} \tag{8} \end{aligned}$$

Power system transient stability simulation-based on the AsDTM method was introduced for the first time by [24]. In using this mathematical tool, the local truncation error at each simulation time step is controlled by setting an acceptable minimum error per unit as illustrated and shown by Equation (8). This enables the AsDTM method to improve the performance efficiency and accuracy of the DTM-based transient stability analysis method. As presented by [24], the accuracy and speed of the transient stability simulation based on AsDTM are investigated in comparison with the classical differential transformation method and the traditional numerical integration method used for IEEE 9 and IEEE 39 test systems. The simulation results reveal that this method improves the simulation speed by 20–44.57% and 83–92% compared with the classical DTM and traditional numerical-integration-based simulation methods, respectively. It is also proven that compared with the DTM-based simulation, the method provides 45.27% to 58.85% and more than 90% accurate simulation results for IEEE 9 and IEEE 39 test systems, respectively.

2.5.2. Descriptions of the Proposed Transient Stability Analysis Based TSI Evaluations

Transient stability analysis-based TS indices evaluation of the scenario is triggered after the fault/event parameters (parameters that represent each credible contingency)

have been determined for all credible contingencies listed and the power system model is initialized. In this paper, an AsDTM-based transient stability analysis method is introduced and used to screen and rank contingencies. At every simulation time step, during the power system transient stability simulation considering each credible contingency, the TSI (AI and SI) is evaluated as the weighted sum of squares of errors derived from state variables and complex bus voltages. Indices evaluated for all listed credible contingencies are related by normalizing them with the largest of all and ranked. Finally, the worst contingency is identified for the next detail assessment. Application of this method significantly improves the performance efficiency as well as robustness of the assessment process. Figure 2 shows a flowchart of the proposed transient stability analysis-based TS indices evaluation algorithm and its descriptions will be presented step by step in this subsection as follows: Where $\psi(k) = DT$ of $\psi(t)$ and $V(k) = DT$ of $v(t)$.

Consider that the state space representation of the power system DAE model equations are as given by Equation (9), where ψ is the state vector, v is the vector of bus voltages, f represents a vector field determined by differential equations on dynamic devices such as synchronous generators and associated controllers, i is the vector valued function on current injections from all generators and load buses, and Y_{bus} is the network admittance matrix.

$$\begin{aligned} \frac{d\psi_j}{dt} &= f(\psi_j, v_j) \\ Y_{bus}v_j &= i(\psi_j, v_j) \end{aligned} \quad (9)$$

where $\psi(t)$ represents the machines and respective controllers state variables such as $\delta_j(t), \omega_j(t), E'_{qj}(t), E'_{dj}(t), V_{rj}(t), V_{fj}(t), E_{fj}(t), P_{chj}(t),$ and $P_{svj}(t)$ and $j = 1, 2, 3, \dots, m$, represent the machine number.

Step 1 Derive DTs of power system DAEs:

Apply the differential transformation to functions given by Equation (9) on both sides, by using transformation rule (g) to obtain Equation (10)

$$\begin{aligned} (k+1)\psi(k+1) &= F(k) = F(\psi(l), V(l)), l = 0 \dots k & (a) \\ Y_{bus}V(k) &= I(k) = I(\psi(l), V(l)), l = 0 \dots k & (b) \end{aligned} \quad (10)$$

The vector valued function $i(\psi, v)$ in Equation (9) represents both generators and load current injections. But here for this specific case, constant impedance loads are considered and are included in the network admittance matrix Y_{bus} . Differential transformation of the network equations including the stator algebraic equation can be derived as given below:

$$\text{Let } y_a = \begin{pmatrix} r_a & -x'_q \\ x'_d & r_a \end{pmatrix}^{-1}, \rho = \begin{pmatrix} \sin\delta & \cos\delta \\ -\cos\delta & \sin\delta \end{pmatrix}, \sigma = \rho y_a, \\ \beta = \rho y_a \rho',$$

And the generator current injection equation is given as Equation (11)

$$\begin{bmatrix} I_x \\ I_y \end{bmatrix} = \left(\sigma \begin{bmatrix} E'_d \\ E'_q \end{bmatrix} - \beta \begin{bmatrix} V_x \\ V_y \end{bmatrix} \right) \quad (11)$$

Using the transformation rule (h & i), differential transformations of ρ , β , and σ are given:

$$\rho(k) = \begin{pmatrix} \varphi(k) & \alpha(k) \\ -\alpha(k) & \varphi(k) \end{pmatrix}, \sigma(k) = \rho(k)y_a, \beta(k) = \rho(k)y_a\rho(k)'$$

Similarly, using transformation rule (d), the differential transformation of the generator current injection equation is

$$\begin{bmatrix} I_x(k) \\ I_y(k) \end{bmatrix} = \left(\sum_{m=0}^k \sigma(m) \begin{bmatrix} E'_d(k-m) \\ E'_q(k-m) \end{bmatrix} - \sum_{m=0}^k \beta(m) \begin{bmatrix} V_x(k-m) \\ V_y(k-m) \end{bmatrix} \right) \quad (12)$$

The load current injection at each bus is represented by

$$\begin{bmatrix} I_x(k) \\ I_y(k) \end{bmatrix} = \text{zeros}(2, 1) \tag{13}$$

And finally, the DTs of the network algebraic equations are

$$\begin{bmatrix} I_{x1}(k) \\ I_{y1}(k) \\ \vdots \\ I_{xi}(k) \\ I_{yi}(k) \\ \vdots \\ I_{xN}(k) \\ I_{yN}(k) \end{bmatrix} = \begin{pmatrix} Y_{11} & \dots & Y_{1i} & \dots & Y_{1N} \\ \vdots & \ddots & \vdots & & \vdots \\ Y_{1i} & \dots & Y_{ij} & \dots & Y_{iN} \\ \vdots & & \vdots & \ddots & \vdots \\ Y_{N1} & \dots & Y_{Nj} & \dots & Y_{NN} \end{pmatrix} \begin{bmatrix} V_{x1}(k) \\ V_{y1}(k) \\ \vdots \\ V_{xi}(k) \\ V_{yi}(k) \\ \vdots \\ V_{xN}(k) \\ V_{yN}(k) \end{bmatrix} \quad I(k) = YV(k) \tag{14}$$

where $i = 1, 2, 3, \dots, N$, and I_{ix} and I_{iy} represent the x and y component of bus i current, v_{ix} & v_{iy} represent x and y component of bus i voltage and

$$Y_{ij} = \begin{pmatrix} G_{ij} & -B_{ij} \\ B_{ij} & G_{ij} \end{pmatrix}, \quad I(k) = \begin{bmatrix} I_{x1}(k) \\ I_{y1}(k) \\ \vdots \\ I_{xi}(k) \\ I_{yi}(k) \\ \vdots \\ I_{xN}(k) \\ I_{yN}(k) \end{bmatrix}, \quad V(k) = \begin{bmatrix} V_{x1}(k) \\ V_{y1}(k) \\ \vdots \\ V_{xi}(k) \\ V_{yi}(k) \\ \vdots \\ V_{xN}(k) \\ V_{yN}(k) \end{bmatrix}$$

Step 2 Solve power series coefficients:

This step is initialized by the initial values of bus voltage $V(0)$ and state variables $\psi(0)$. The main task here is to solve power series coefficients $\psi(k)$ and $V(k)$ ($k \geq 1$) from the $(k - 1)$ th order coefficients, as indicated by two circled numbers in Figure 3. Thus, any order coefficients are solvable from $\psi(0), V(0)$.

The coefficients of state variables $\psi(k)$ for differential equations are derived from Equation (10)a recursively from $\psi(1)$ up to $\psi(k)$, as shown in Figure 3. But solving the coefficients of algebraic variables, bus voltage $V(k)$ is not straightforward since $V(k)$ appears on both sides as we can observe from Equation (10)b. If ZIP load models are considered, the current injection equations for constant power and constant current load portions of the ZIP load are non-linear and these will be turned to linear in terms of their coefficients; the proof is given in [21]. Since the constant impedance load is considered in this paper, the differential transforms of generator current injection given by Equation (15) can be rewritten as Equation (16) below.

$$\begin{bmatrix} I_x(k) \\ I_y(k) \end{bmatrix} = \left(\sum_{m=0}^k \sigma(m) \begin{bmatrix} E'_d(k-m) \\ E'_q(k-m) \end{bmatrix} - \sum_{m=1}^k \beta(m) \begin{bmatrix} V_x(k-m) \\ V_y(k-m) \end{bmatrix} \right) \dots - \beta(0) \begin{bmatrix} V_x(k) \\ V_y(k) \end{bmatrix} \tag{15}$$

Let

$$B_g = \sum_{m=0}^k \sigma(m) * \begin{bmatrix} E'_d(k-m) \\ E'_q(k-m) \end{bmatrix} - \sum_{m=1}^k \beta(m) * \begin{bmatrix} V_x(k-m) \\ V_y(k-m) \end{bmatrix}$$

$$A_g = \beta(0)$$

$$\begin{bmatrix} I_x(k) \\ I_y(k) \end{bmatrix} = A_g \begin{bmatrix} V_x(k) \\ V_y(k) \end{bmatrix} + B_g \quad \text{i.e.} \quad I(k) = A_g V(k) + B_g \tag{16}$$

Since the load current injection is zero, let A_l represent zeros (2,2), B_l represents zeros (2,1) at each of the n buses, $A = A_g + A_l$ & $B = B_g + B_l$ for machine buses and $A = A_l$ & $B = B_l$ at $(n-m)$ buses then A represents $(2 \times n)$ by $(2 \times n)$ matrixes and B represents $(2 \times n)$ by 1 column vector. Therefore, the current injections into the network from all the buses can be expressed as Equation (17) below

$$I(k) = AV(k) + B \tag{17}$$

where $I(k)$ and $V(k)$ are as given for Equation (14)

Considering constant impedance loads, the coefficients of bus voltages $V(k)$ for all the network buses and coefficients of state variables $\psi(k)$ are solved from Equation (18) from a-c recursively from $\psi(1)$ up to $\psi(k)$ and $V(1)$ up to $V(k)$.

$$\begin{aligned} \psi(k) &= \frac{1}{k} F(\psi(1), V(1)), \quad 1 = 0 \dots k - 1 & \text{(a)} \\ Y_{\text{bus}} V(k) &= AV(k) + B & \text{(b)} \\ V(k) &= (Y_{\text{bus}} - A)^{-1} B & \text{(c)} \end{aligned} \tag{18}$$

Step 3 Inverse DT on $\psi(k)$ and $V(k)$.

Apply inverse DT to $\psi(k)$ and $V(k)$ to obtain the DTM-based solution of power system DEAs in (20) a&b, where $\psi(k)$ and $\psi(t)$ represent $\delta_i(k)$, $\omega(k)_i E'_{qi}(k)$, $E'_{di}(k)$, $V_i(k)$, $V_{fi}(k)$, $P_{chi}(k)$, $P_{svi}(k)$ and $E_{fi}(k)$ & $\delta_i(t)$, $\omega(t)_i E'_{qi}(t)$, $E'_{di}(t)$, $V_i(t)$, $V_{fi}(t)$, $P_{chi}(t)$, $P_{svi}(t)$ and $E_{fi}(t)$ respectively. & $i = 1, 2, 3, \dots, m$, represent the machine number

$$\begin{aligned} \psi(t) &= \sum_{m=0}^k \psi(m) t^m & \text{(a)} \\ v(t) &= \sum_{m=0}^k V(m) t^m & \text{(b)} \end{aligned} \tag{19}$$

Step 4 Determine the new step size (hnew):

As described in Section 2.5.1 above, we can estimate the simulation step size that ensures the prescribed local admissible error by using just one of the coefficient terms without any further calculation. The equation to calculate the step size (h) given by Equation (8) above is adopted and applied for power system transient stability analysis, as described below.

Let M_{st} , E_{Xst} , and T_{Gst} be the matrix of generators, exciters, and turbine governor state variables, respectively. If m and N represent the number of machines and state variables, respectively, the size of each matrix is equal to $m \times N$. Consider also the tolerable local solution error $\partial > 0$. The order of DTM, k , is given and fixed at the beginning of the simulation. Therefore, since all order coefficient terms of state variables and all the network bus voltages are known at this stage, the new step size (h_{new}) will be determined. In this paper, an admissible local solution error of $\partial = 10^{-6}$ per unit is considered. Therefore, we can calculate the new step size h using the following two steps:

- I. Determine the maximum of the absolute value of the last coefficient terms of all the variables as in Equation (20):

$$E = \text{Max}[\text{Max}(\text{Max}(|Mst(k)|), \text{Max}(\text{Max}(|EXst(k)|), \dots \text{Max}(\text{Max}(|TGst(k)|), \text{Max}(|V(k)|)))] \tag{20}$$

- II. Next, evaluate the new step size h_{new} by using Equation (21):

$$h_{\text{new}} = \left(\left(\frac{\partial}{E} \right)^{\frac{1}{k}} \right)^{\leq \text{max step size (hmax)}} \tag{21}$$

Step 5 Check for disturbance or event, and if any, determine the new (Y)matrix and reinitialize bus voltages.

Step 6 Increment the simulation time t as $t_{i+1} = t_i + h_{new}$ (where i represents the number of time nodes, separated by the length of every time window).

Step 7 Determining transient stability indices (TSI)

The TSI of each considered contingency is determined in terms of the dynamic performance response at each machine bus. The dynamic performance response at each machine bus is determined in terms of the machine state and algebraic variable values deviation from their respective steady-state conditions. When a power system is subjected to a large disturbance, the algebraic variables change instantly while the machine state variables may need some transient time to change values. Upon clearing, the variables are expected to return to their initial operating values or new and acceptable steady state values. However, this is not always the case due to the severity of that disturbance.

In this paper, transient stability index values, such as SI and AI representing the machine-related state variables and machine bus complex voltage deviations from steady state conditions, respectively, are used to identify and list contingencies according to their severity. For each contingency in the list, these deviations are expressed as the weighted sum of squares of error of the machine state and non-state variables, complex bus voltages at each simulation time step [8] as defined by Equation (22).

$$\begin{aligned}
 SI_{new} &= SI_{prev} + \left(\frac{\sum_{i=1}^m \sum_{j=1}^l W_{ij} (\psi_{ij}(t) - \psi_{ij}(t_0))^2}{m} \right) * h \\
 AI_{new} &= AI_{prev} + \left(\frac{\sum_{i=1}^m \sum_{j=1}^l W_{ij} (v_{ij}(t) - v_{ij}(t_0))^2}{m} \right) * h
 \end{aligned} \tag{22}$$

where:

h = the new step-size, v = complex machine bus voltage, ψ = machine's state variables

SI_{new} = new transient stability index values of machine related state variables

SI_{prev} = previous transient stability index values of machine related state variables

AI_{new} = new transient stability index values of machine bus complex voltage

AI_{prev} = previous transient stability index values of machine bus complex voltage

W_{ij} = weight associated with the state and algebraic variables

l = the number of the state or algebraic variables.

The transient stability index values of state and algebraic variables ψ and v , respectively, and the step-size (h) in the above equations are obtained from the power system transient stability simulation results at each simulation time step. These indices can be evaluated starting from any time as required during the simulation period. Finally, indices evaluated for all listed credible contingencies are related by normalizing them with the largest of all.

Step 8 Using the time domain solutions $\psi(t)$ and $v(t)$ (step 3, above) as initial values of the state variables and bus voltages for the next simulation time window, respectively, repeat steps 2 to 8 until the end of the simulation period (T).

2.6. Contingencies Are Ranked and the Worst Contingency Is Identified

For each considered contingency case, respective transient stability indices are evaluated. Finally, each of the transient stability indices are normalized with the largest of all the indices and listed in descending order. The contingency in the top position is the most critical contingency identified and the contingency in the bottom position is the least critical contingency.

3. Case Studies and Results

3.1. Test System, Cases, and Setup

3.1.1. Test System

Two test systems are employed to validate the proposed screening approach. The first test system is the 9-bus system, which consists of nine buses and three machines. The second test system is the 39-bus system, which consists of 39 buses and 10 machines, as shown by Figure 4 below. The loads are modeled as constant impedances in the time domain simulation. The generators are represented by a two-axis fourth-order model. They all have a Type_1 excitation and voltage regulation system as well as a turbine/governor model.

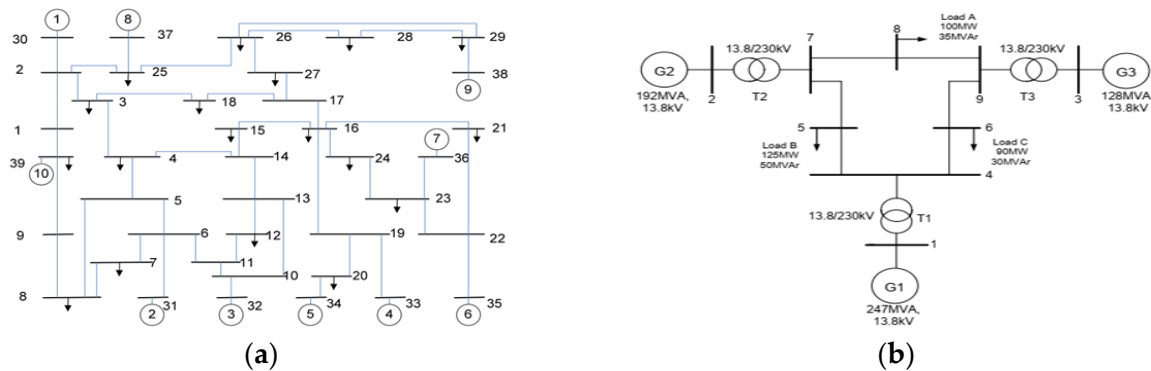


Figure 4. One-line diagram of (a) New England 39-bus system; (b) IEEE 9-bus system [24].

3.1.2. Test Cases

For the purpose of testing the proposed fast contingency screening method, a set of contingencies are defined. For both systems, three phase bus faults are considered. This located at 6 buses (non-generator buses) for the first test system and 29 buses (similarly, non-generator buses) for the second test system. A susceptance of 10^{-10} is considered enough to bring zero impedance bus faults [27]. This fault is added to the network admittance matrix for every non-generator bus in sequential order (one after the other). In this paper, the fault is cleared only by removing the added fault parameters from the respective bus admittance matrix without isolating the faulted bus itself so that the network structure is not changed.

3.1.3. Test Setup

The tests are carried out on a standard laptop with the following characteristics: Intel (TM) i5-5200U CPU @ 2.20 GHz, 8 GB RAM, running on a 64-bit operating system, with a x64-based processor. The transient stability analysis-based TSI evaluations were carried out using the tools/codes developed by using the proposed AsDTM on MATLAB R2017b [28]. MATPOWER 7.1 [29] version software was utilized. The CPU time included all steps of the transient stability analysis-based TSI evaluation processes. MATPOWER is open-source software for power flow analysis and run on a MATLAB environment. This power system analysis software does not employ a graphical representation of a power system. Instead, the power system data were prepared in a table format specific to MATPOWER. Any functions of the MATPOWER can easily be accessed by functions developed on MATLAB editor. These include MATLAB functions that load and call for dynamic and static data file of simulation cases (case file), MATPOWER output interface functions, functions for initializing dynamic systems, model libraries for all dynamic systems, solver functions file (algorithms for computation), and functions for plotting simulation results. Power flow analysis was performed using MATPOWER.

3.2. Assessment Results and Discussion

To validate the proposed contingency screening and ranking method, three-phase short-circuit faults located at 6 buses (non-generator buses) for IEEE 9-bus test system and 29 buses (similarly, non-generator buses) for the 39-bus test system are used. To analyze

their impacts, each fault is triggered at 0.6 s and cleared at two different fault clearing times. TSI for each faulted bus is evaluated, first by considering the 0.15 s (150 ms) fault clearing time and next by considering the 0.25 s (250 ms) fault clearing time. During both scenarios, the evaluated TSI are ranked and plotted. In both cases, the accuracy and performance of the proposed method are validated using the assessment results based on the traditional numerical method (fourth-order Runge–Kutta (Rk4) with step size $h = 0.001$ s) as benchmarks. For this purpose, the differential transformation (DT) order $k = 14$ is used for both test systems with both DTM and AsDTM simulation methods.

Two types of TS indices are evaluated for each credible contingency during transient stability analysis at each assessment time step. These indices were evaluated based on the machine's state variables (as rotor angle deviations(δ), angular speed($\dot{\omega}$), etc.); analysis results are represented as state variable indices (SI) and those evaluated based on the machine's bus complex bus voltages (such as bus voltage magnitude (V) and voltage angle(θ)) analysis results are represented as algebraic variable indices (AI).

3.2.1. Validation of the Accuracy of the Proposed Method

In the following sub-section, the accuracy of the proposed method is validated with respect to the TS indices evaluated using transient stability analysis based on a traditional numerical method (fourth order Runge–Kutta (Rk4)) as a benchmark. Tests are performed considering two scenarios. During the first scenario, contingencies are analyzed and ranked considering a 150 ms fault clearing time and the next scenario by considering a 250 ms fault clearing time. The TSI evaluated based on a fourth order Runge–Kutta Rk4 (reference method), the proposed AsDTM, and the classical DTM methods using both test systems are plotted as shown by Figures 5a,b and 6a,b below. The TSI results evaluated based on the proposed method, and those evaluated from the classical DTM method (with a fixed step-size of $h = 0.0125$ s) are ranked and compared with the benchmark results as given in Tables 1–4 below. As one can clearly observe from the plots given by Figures 5a,b and 6a,b, the TSI (AI and SI) results evaluated based on the proposed method for the 150 ms fault clearing time indicate that the most and least critical situations are when there is a three phase short-circuit fault at buses 22 and 12, respectively, for the 39-bus test system and at buses 8 and 5, respectively, for the 9-bus test system. These results strongly agree with the most and least critical buses identified based on the Rk4 (benchmark) for both test cases as shown by Figures 5a,b and 6a,b below. But the plots of the TSI evaluated based on the classical DTM method indicate that the most and least critical situations are when there is a three-phase short-circuits fault at buses 22 and 9, respectively, for the 39-bus test system. This result shows that the least critical situation identified by using the classical DTM method is completely different from the benchmark result.

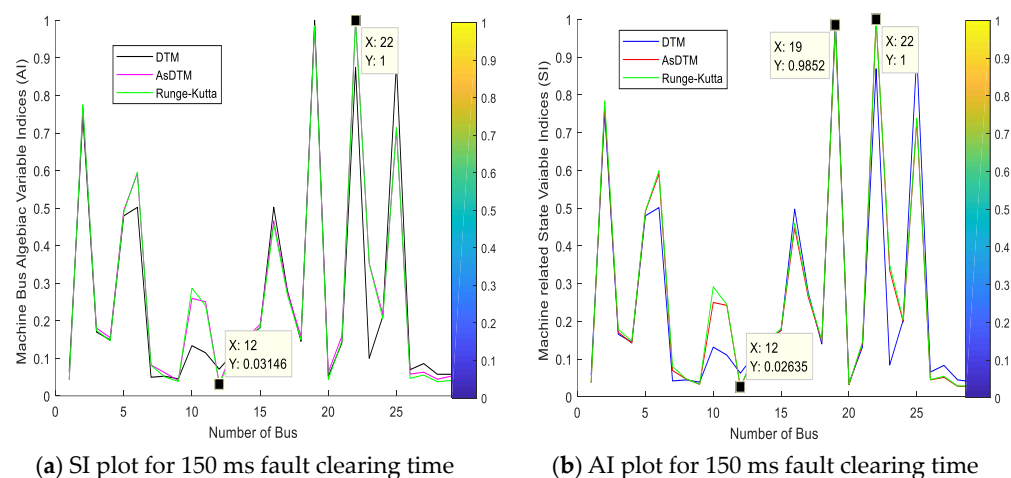
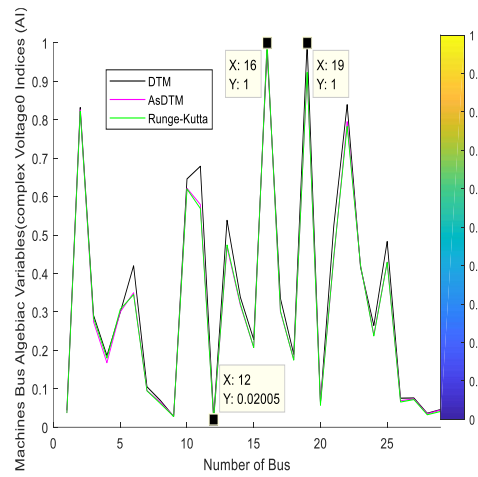
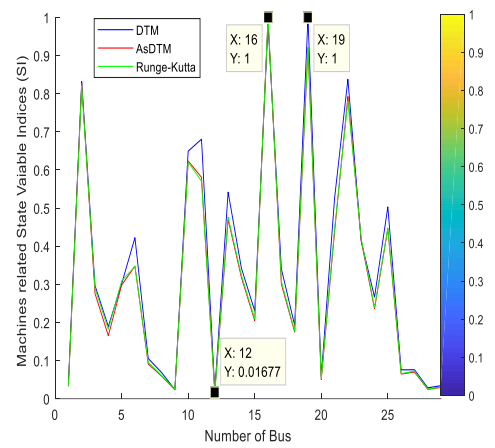


Figure 5. Cont.

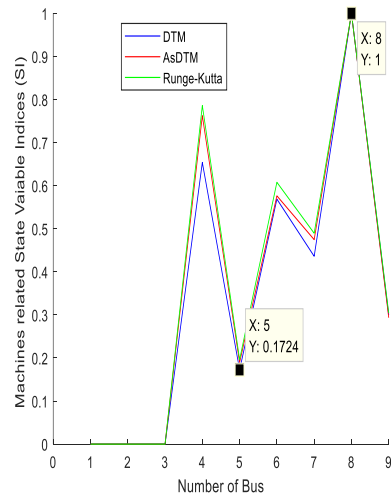


(c) SI plot for 250 ms fault clearing time

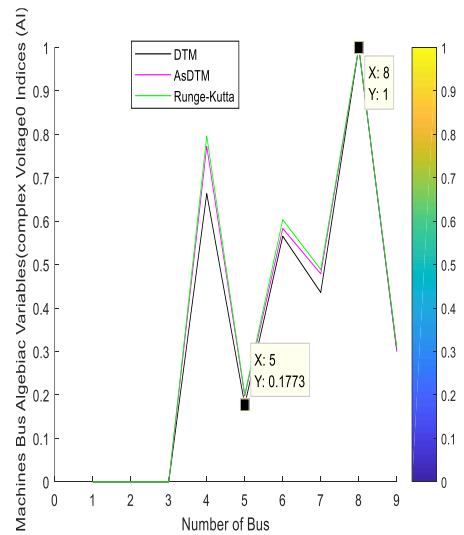


(d) AI plot for 250 ms fault clearing time

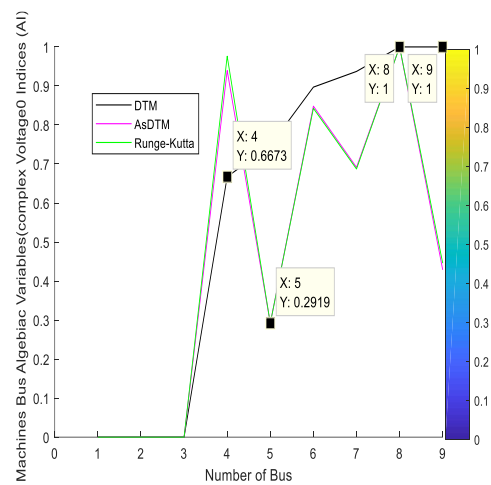
Figure 5. SI and AI plots of 39-bus test system.



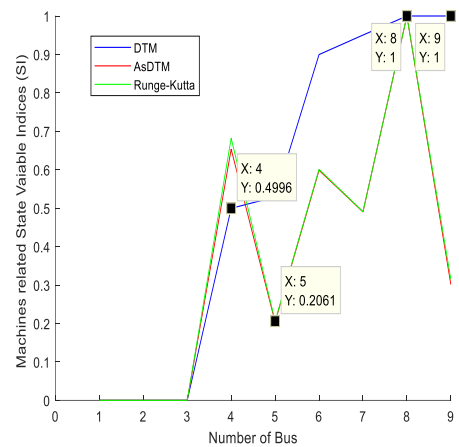
(a) SI plot for 150 ms fault clearing time



(b) AI plot for 150 ms fault clearing time



(c) SI plot for 250 ms fault clearing time



(d) SI plot for 250 ms fault clearing time

Figure 6. SI and AI plots of 9-bus test system.

Table 1. Three-phase short-circuit on each non-generator buses of 39-bus test system and each cleared after 150 ms.

Cont. Ranked Using TSI Evaluated Based on Numerical Integration Method (Benchmarks)		Cont. Ranked Using TSI Evaluated Based on AsDTM Method		Con. Ranked Using TSI Evaluated Based on DTM Method	
Bus No	Rank	Bus No	Rank	Bus No	Rank
Bus 22	1	Bus 22	1	Bus 22	1
Bus 19	2	Bus 19	2	Bus 19	2
Bus 2	3	Bus 2	3	Bus 2	3
Bus 25	4	Bus 25	4	Bus 25	4
Bus 6	5	Bus 6	5	Bus 6	5
Bus 5	6	Bus 5	6	Bus 16	6
Bus 16	7	Bus 16	7	Bus 5	7
Bus 23	8	Bus 23	8	Bus 23	8
Bus 10	9	Bus 10	9	Bus 10	9
Bus 17	10	Bus 17	10	Bus 17	10
Bus 11	11	Bus 11	11	Bus 15	11
Bus 24	12	Bus 24	12	Bus 11	12
Bus 15	13	Bus 15	13	Bus 24	13
Bus 3	14	Bus 3	14	Bus 3	14
Bus 14	15	Bus 18	15	Bus 21	15
Bus 18	16	Bus 14	16	Bus 18	16
Bus 4	17	Bus 4	17	Bus 14	17
Bus 21	18	Bus 21	18	Bus 4	18
Bus 13	19	Bus 13	19	Bus 13	19
Bus 7	20	Bus 7	20	Bus 27	20
Bus 27	21	Bus 27	21	Bus 26	21
Bus 8	22	Bus 8	22	Bus 8	22
Bus 26	23	Bus 26	23	Bus 1	23
Bus 1	24	Bus 1	24	Bus 7	24
Bus 9	25	Bus 9	25	Bus 29	25
Bus 20	26	Bus 20	26	Bus 28	26
Bus 28	27	Bus 28	27	Bus 12	27
Bus 29	28	Bus 29	28	Bus 20	28
Bus 12	29	Bus 12	29	Bus 9	29

Table 2. Three-phase short-circuit on each non-generator buses of 9-bus test system and each cleared after 150 ms.

Cont. Ranked Using TSI Evaluated Based on Numerical Integration Method (Benchmarks)		Cont. Ranked Using TSI Evaluated Based on AsDTM Method		Con. Ranked Using TSI Evaluated Based on DTM Method	
Bus No	Rank	Bus No	Rank	Bus No	Rank
Bus 8	1	Bus 8	1	Bus 8	1
Bus 4	2	Bus 4	2	Bus 4	2
Bus 6	3	Bus 6	3	Bus 6	3
Bus 7	4	Bus 7	4	Bus 7	4
Bus 9	5	Bus 9	5	Bus 9	5
Bus 5	6	Bus 5	6	Bus 5	6

Similarly, from the plots given by Figures 5c,d and 6c,d, the TSI (AI and SI) evaluated based on the proposed method for the 250 ms fault clearing time indicate that the most and least critical situations are when there is a three-phase short-circuit fault at buses 16 and 12, respectively, for the 39-bus test system and at buses 8 and 5, respectively, for the 9-bus test system. These results again strongly agree with the most and least critical buses identified based on the reference method for both test cases. But the plots of the TSI based

on the classical DTM method indicate that the most and least critical situations are when there is a three-phase short-circuit fault at buses 19 and 12, respectively, for the 39-bus test system and at buses 8 or 9 and 4, respectively, for the 9-bus test system. These results show that the most and least critical situations identified by using the classical DTM method are different from those identified by the benchmark method. Therefore, more accurate results are found by using the proposed contingency screening and ranking method.

Table 3. Three-phase short-circuit on each non-generator buses of 39-bus test system and each cleared after 250 ms.

Cont. Ranked Using TSI Evaluated Based on Numerical Integration Method (Benchmarks)		Cont. Ranked Using TSI Evaluated Based on AsDTM Method		Con. Ranked Using TSI Evaluated Based on DTM Method	
Bus No	Rank	Bus No	Rank	Bus No	Rank
Bus 16	1	Bus 16	1	Bus 19	1
Bus 19	2	Bus 19	2	Bus 16	2
Bus 2	3	Bus 2	3	Bus 22	3
Bus 22	4	Bus 22	4	Bus 2	4
Bus 10	5	Bus 10	5	Bus 11	5
Bus 11	6	Bus 11	6	Bus 10	6
Bus 13	7	Bus 13	7	Bus 13	7
Bus 25	8	Bus 25	8	Bus 21	8
Bus 21	9	Bus 21	9	Bus 25	9
Bus 23	10	Bus 23	10	Bus 6	10
Bus 6	11	Bus 6	11	Bus 23	11
Bus 14	12	Bus 14	12	Bus 14	12
Bus 5	13	Bus 5	13	Bus 17	13
Bus 17	14	Bus 17	14	Bus 12	14
Bus 3	15	Bus 3	15	Bus 3	15
Bus 24	16	Bus 24	16	Bus 24	16
Bus 15	17	Bus 15	17	Bus 15	17
Bus 4	18	Bus 18	18	Bus 18	18
Bus 18	19	Bus 4	19	Bus 4	19
Bus 7	20	Bus 7	20	Bus 24	20
Bus 27	21	Bus 27	21	Bus 27	21
Bus 26	22	Bus 26	22	Bus 26	22
Bus 8	23	Bus 8	23	Bus 8	23
Bus 20	24	Bus 20	24	Bus 20	24
Bus 1	25	Bus 1	25	Bus 1	25
Bus 29	26	Bus 29	26	Bus 29	26
Bus 28	27	Bus 28	27	Bus 28	27
Bus 9	28	Bus 9	28	Bus 9	28
Bus 12	29	Bus 12	29	Bus 12	29

Table 4. Three-phase short-circuit on each non-generator buses of 9-bus test system and each cleared after 250 ms.

Cont. Ranked Using TSI Evaluated Based on Numerical Integration Method (Benchmarks)		Cont. Ranked Using TSI Evaluated Based on AsDTM Method		Con. Ranked Using TSI Evaluated Based on DTM Method	
Bus No	Rank	Bus No	Rank	Bus No	Rank
Bus 8	1	Bus 8	1	Bus 8 & Bus 9	1
Bus 4	2	Bus 4	2	Bus 7	2
Bus 6	3	Bus 6	3	Bus 6	3
Bus 7	4	Bus 7	4	Bus 5	4
Bus 9	5	Bus 9	5	Bus 4	5
Bus 5	6	Bus 5	6	-	6

In addition, Figures 5a–d and 6a–d representing the SI and AI plots, where the quality of the plot results obtained with the AsDTM and DTM methods used the convergence criterion, the measure of which is the concurrency of trajectories rout corresponding to two compared solutions. The best convergence was found for the AsDTM-based SI and AI plots. This implies that the AsDTM-based TSI evaluation gives more accurate results. On the other hand, since the shapes of the trajectories obtained by both the DTM and AsDTM methods were the same as the reference trajectory for the first scenario (Figures 5a,b and 6a,b) we can conclude that both the DTM and AsDTM methods are numerically stable. However, when we observe the TSI plots for the second scenario (for the 250 ms fault clearing time), specially Figure 6c,d show that the DTM method is not numerically stable as the network complexity decreases and fault clearing time increases.

Tables 1–4 below give contingencies ranked using their respective TSI evaluated based on the benchmark, classical DTM and the proposed AsDTM methods considering both 150 ms and 250 ms fault clearing by using both test systems. From the summary and the results given in Table 5, in all cases the proposed AsDTM-based contingency screening and ranking method provides 93% accurate results.

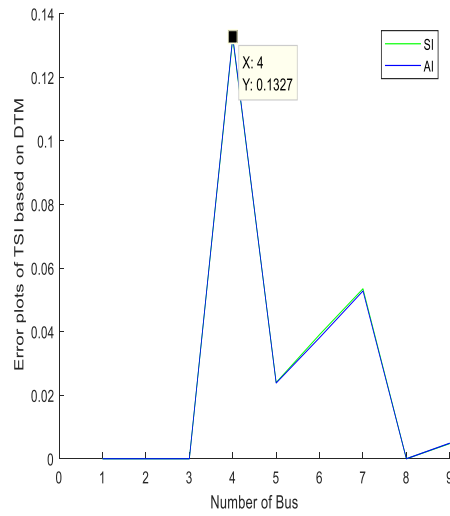
Table 5. Summary of the accuracy of the ranked contingencies based on DTM and the proposed AsDTM methods compared with the benchmark results.

Fault Cleared	Accuracy of Contingencies Ranked Using TSI Evaluated Based on AsDTM Method in %		Accuracy of Contingencies Ranked Using TSI Evaluated Based on DTM Method in %	
	For 39-Bus Test System	For 9-Bus Test System	For 39-Bus Test System	For 9-Bus Test System
150 ms	93	100	41.38	100
250 ms	93	100	44.82	16.67

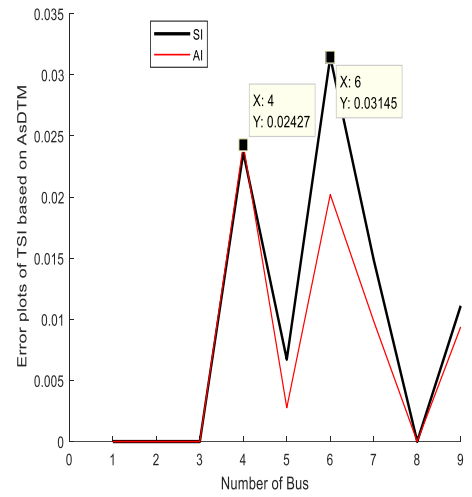
Compared with the benchmark results, the range of accuracy of assessment results based on the proposed AsDTM and the classical DTM methods are summarized as given in Table 5 below.

From the results summary given in Table 5 above, we can conclude that the proposed contingency screening and ranking method is more accurate compared with the DTM method. The increase in the fault clearing time also has no influence on the accuracy of the proposed AsDTM method. Further, as the complexity or sizes of the network decrease the proposed method is as accurate as the reference method. But we can simply observe from the assessment results given in Tables 1–5 that as the network size as well as the fault clearing time increase the probability that the classical DTM method can identify the most critical contingency is almost null.

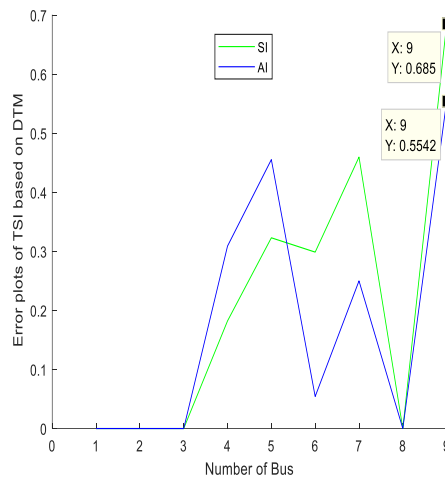
Even though the most and least critical buses screened out based on the proposed method are the same as the benchmark results (evaluated based on the Rk4 method) in all cases, the magnitudes of the evaluated TS indices (SI and AI) for the three-phase short-circuit at all non-generator buses for both test cases are not the same as the benchmark results. Figures 7a–d and 8a–d below show the error plots of the AsDTM- and DTM-based evaluated transient stability indices. As can be seen from Figures 7 and 8a–d, the magnitudes of the generated SI and AI error by the DTM-based evaluation method are 0.1664 and 0.1619, respectively, for the 39-bus test system and 0.1327 for the 9-bus test system, when the fault is cleared after 150 ms in both cases. Similarly, the magnitudes of the generated SI and AI error by the proposed AsDTM-based evaluation method are 0.0418 and 0.02753, respectively, for the 39-bus test system and 0.03145 and 0.02427, respectively, for the 9-bus test system when the fault is cleared after 150 ms in both cases.



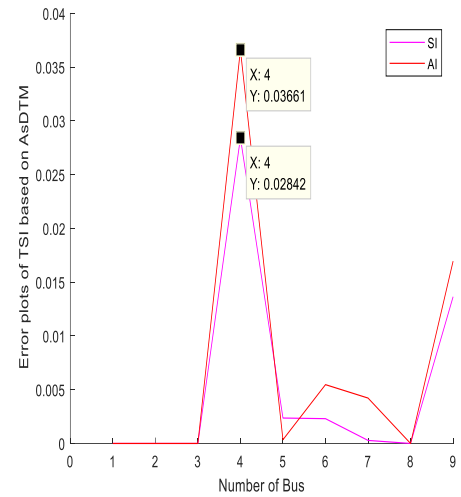
(a) Plots TSI evaluated based on DTM for fault clearing time of 150 ms



(b) Plots TSI evaluated based on AsDTM for fault clearing time of 150 ms

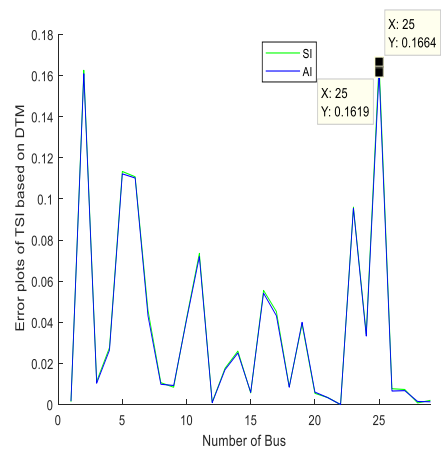


(c) Plots TSI evaluated based on DTM for fault clearing time of 250 ms

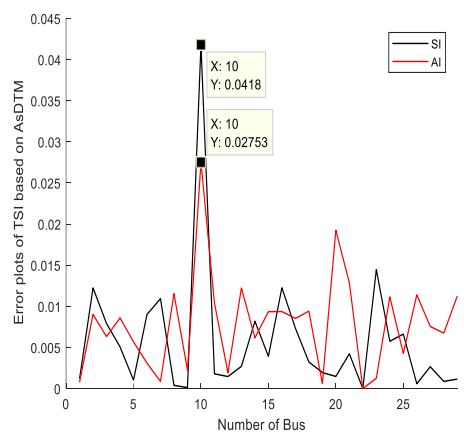


(d) Plots TSI evaluated based on AsDTM for fault clearing time of 250 ms

Figure 7. DTM- and AsDTM-based SI and AI error plots for 9-bus test system.

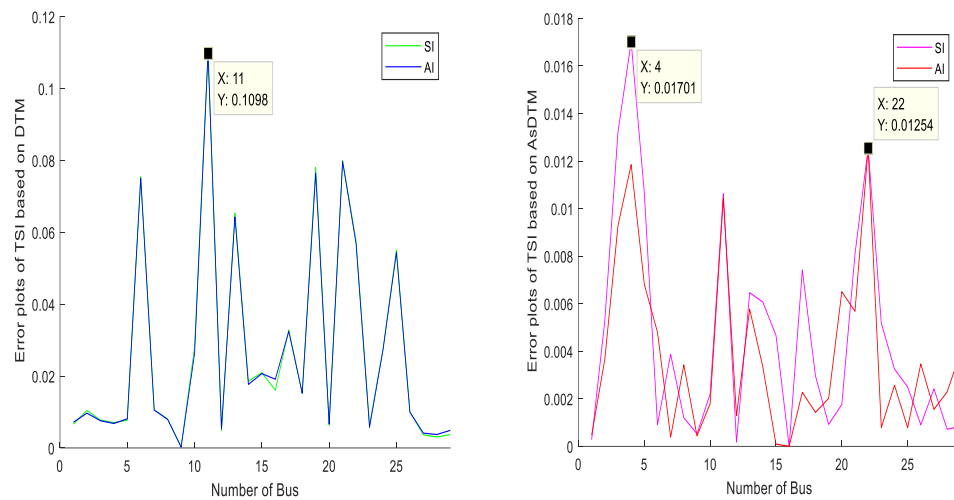


(a) Plots TSI evaluated based on DTM for fault clearing time of 150 ms



(b) Plots TSI evaluated based on AsDTM for fault clearing time of 150 ms

Figure 8. Cont.



(c) Plots TSI evaluated based on DTM for fault clearing time of 250 ms (d) Plots TSI evaluated based on AsDTM for fault clearing time of 250 ms

Figure 8. DTM- and AsDTM-based SI and AI error plots for 39-bus test system plots.

Similarly, when the fault is cleared after 250 ms, the magnitudes of the generated SI and AI error by the proposed AsDTM-based evaluation method are 0.01701 and 0.01254, respectively, for the 39-bus test system and 0.03661 and 0.02842, respectively, for the 9-bus test system and the magnitudes of the generated SI and AI error by the DTM-based evaluation method are 0.1098 for the 39-bus test system and 0.685 and 0.5542 for the 9-bus test system, respectively.

Compared to the proposed method, the magnitude of the SI and AI error generated by the classical DTM-based evaluation method is relatively greater. This shows that more accurate indices are evaluated based on the proposed AsDTM method. A summary of the TS indices error magnitude resulted from using AsDTM and DTM assessment methods relative to the benchmark results are given in Table 6 below.

Table 6. TSI error by AsDTM and DTM methods relative to the benchmark results.

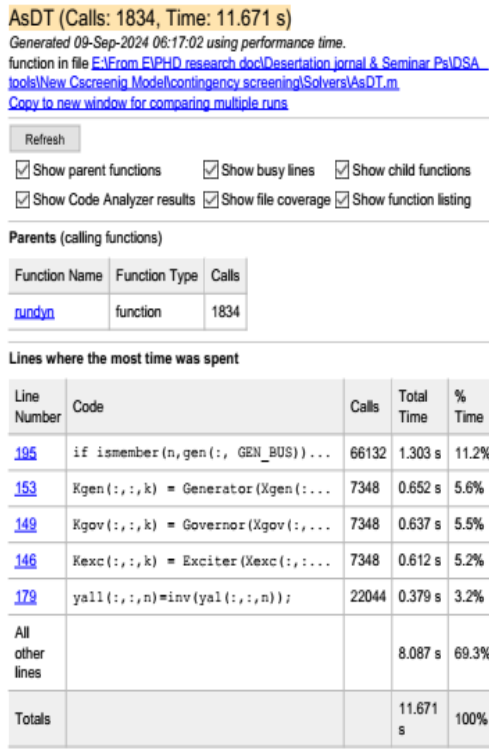
Test System	Fault Cleared After	Assessment Method	Maximum TSI Error	
			SI	AI
9 bus	150 ms	AsDTM	0.03145	0.02427
		DTM	0.1327	0.1327
	250 ms	AsDTM	0.03661	0.02842
		DTM	0.685	0.5542
39 bus	150 ms	AsDTM	0.0418	0.02753
		DTM	0.1664	0.1619
	250 ms	AsDTM	0.01701	0.01254
		DTM	0.1098	0.1098

From Table 6, we can conclude that using the proposed AsDTM method in terms of the DTM method for contingency screening and ranking improves the accuracy of the TSI evaluation results by 74% up to 83% if the fault is cleared after 150 ms and by 84% up to 94% if the fault is cleared after 250 ms. All the test and analysis results given above prove that the proposed AsDTM method of contingency screen ranking provides more accurate results.

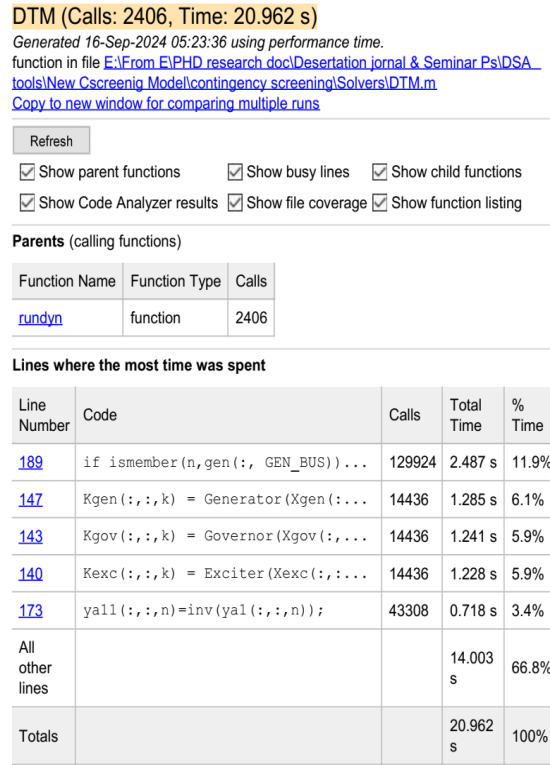
3.2.2. Validation of the Assessment Speed of the Proposed Method

Figures 9a–c and 10a–c show the total elapsed time to evaluate TS indices for contingency screening and ranking based on AsDTM, DTM, and Rk4 methods using both the 39-bus and the 9-bus test system. The total assessment times required to evaluate TS indices

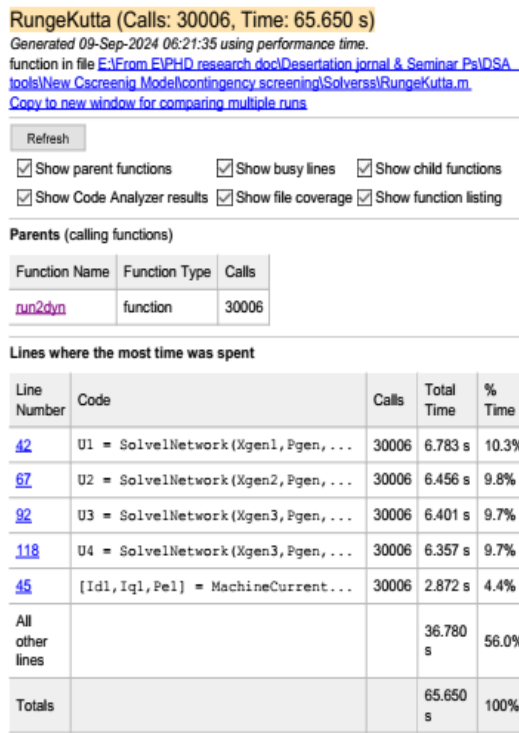
based on AsDTM, DTM, and Rk4 methods are 11.671 s, 20.962 s, and 65.65 s, respectively, for the 9-bus test system and 194.084 s, 279.047 s, and 768.062 s, respectively, for the 39-bus test system.



(a)



(b)



(c)

Figure 9. Elapsed time (a) for AsDTM-based TSI evaluation (b) for DTM-based TSI evaluation (c) for Rk4-based TSI evaluation, of 9-bus test system.

AsDT (Calls: 10770, Time: 194.086 s)

Generated 16-Sep-2024 05:48:44 using performance time.

function in file [E:\From E\PHD_research doc\Desertation jornal & Seminar Ps\DSA_tools\New Cscreenig Model\contingency screening\Solvers\AsDT.m](#)
[Copy to new window for comparing multiple runs](#)

Refresh

Show parent functions
 Show busy lines
 Show child functions
 Show Code Analyzer results
 Show file coverage
 Show function listing

Parents (calling functions)

Function Name	Function Type	Calls
rundyn	function	10770

Lines where the most time was spent

Line Number	Code	Calls	Total Time	% Time
195	if ismember(n,gen(:, GEN_BUS))...	1682382	30.466 s	15.7%
202	Vbus(:,l,k)=(Y-A)\B(:,l,k);	43138	8.814 s	4.5%
101	if ismember(n,gen(:, GEN_BUS))...	420030	7.635 s	3.9%
179	yall(:,:,n)=inv(yal(:,:,n));	431380	6.174 s	3.2%
113	vxy0(2*I-1,l,k)= vx(I,l,k);	420030	4.904 s	2.5%
All other lines			136.094 s	70.1%
Totals			194.086 s	100%

(a)

DTM (Calls: 11629, Time: 279.047 s)

Generated 16-Sep-2024 05:49:38 using performance time.

function in file [E:\From E\PHD_research doc\Desertation jornal & Seminar Ps\DSA_tools\New Cscreenig Model\contingency screening\Solvers\DTM.m](#)
[Copy to new window for comparing multiple runs](#)

Refresh

Show parent functions
 Show busy lines
 Show child functions
 Show Code Analyzer results
 Show file coverage
 Show function listing

Parents (calling functions)

Function Name	Function Type	Calls
rundyn	function	11629

Lines where the most time was spent

Line Number	Code	Calls	Total Time	% Time
189	if ismember(n,gen(:, GEN_BUS))...	2721186	48.237 s	17.3%
196	Vbus(:,l,k)=(Y-A)\B(:,l,k);	69774	13.757 s	4.9%
176	Temp=Temp+(taw(:,:,n,m)*(rt(:,...	2442090	10.526 s	3.8%
173	yall(:,:,n)=inv(yal(:,:,n));	697740	9.991 s	3.6%
95	if ismember(n,gen(:, GEN_BUS))...	453531	8.104 s	2.9%
All other lines			188.431 s	67.5%
Totals			279.047 s	100%

(b)

RungeKutta (Calls: 145029, Time: 768.962 s)

Generated 09-Sep-2024 07:32:23 using performance time.

function in file [E:\From E\PHD_research doc\Desertation jornal & Seminar Ps\DSA_tools\New Cscreenig Model\contingency screening\Solvers\RungeKutta.m](#)
[Copy to new window for comparing multiple runs](#)







Refresh

Show parent functions
 Show busy lines
 Show child functions
 Show Code Analyzer results
 Show file coverage
 Show function listing

Parents (calling functions)

Function Name	Function Type	Calls
run2dyn	function	145029

Lines where the most time was spent

Line Number	Code	Calls	Total Time	% Time	Time Plot
42	U1 = SolveNetwork(Xgen1,Pgen,...	145029	128.832 s	16.8%	
67	U2 = SolveNetwork(Xgen2,Pgen,...	145029	125.069 s	16.3%	
92	U3 = SolveNetwork(Xgen3,Pgen,...	145029	124.610 s	16.2%	
118	U4 = SolveNetwork(Xgen3,Pgen,...	145029	124.526 s	16.2%	
45	[Idl,Iq1,Pe1] = MachineCurrent...	145029	19.972 s	2.6%	
All other lines			245.953 s	32.0%	
Totals			768.962 s	100%	

(c)

Figure 10. Elapsed time (a) for AsDTM-based TSI evaluation (b) for DTM-based TSI evaluation (c) for Rk4-based TSI evaluation, of 9-bus test system.

Compared with DTM and Rk4, the proposed AsDTM-based contingency screening and ranking method improves the performance efficiency (performance speed) by 44.32% and 82.22% for the 9-bus test system and 30.45% and 74.73% for the 39-bus test system, respectively.

Therefore, from the above assessment and simulation results, compared to the conventional Runge–Kutta (Rk4) and the classical DTM methods of contingency screening and

ranking the proposed method improves the assessment speed by more than 74.73% and 30.45%, respectively. Compared to the classical DTM methods of contingency screening and ranking, the proposed method improves the accuracy of the resulting transient stability indices by more than 74%. These results strongly indicate that the proposed contingency screening and ranking method is fast and robust.

A near-real-time DSA cycle time should be short enough for the results to be still meaningful when the evaluation is completed, i.e., in the order of 10 to 15 min [1]. For example, performing a time domain simulation of 5000 contingencies using PowSim for 30 s each on the full UK National Grid Control (NGC) system takes approximately 11.5 h using one computing device. Using a similar computing device with the method of contingency screening proposed in this paper considering only 74% improvement in performance efficiency, the total assessment/simulation time is reduced to 4.14 h. This indicates that compared to the traditional numerical integration method, the proposed method performs with a smaller number of parallel computing devices to complete the whole assessment/simulation processes before the DSA cycle time. Therefore, we can conclude that the proposed contingency screening and ranking method is faster.

4. Conclusions and Future Work

Modern society is very dependent on the availability of electrical energy; therefore, a reliable electricity supply is foundational to all economic and societal activities. To supply this continuously growing demand, the size and complexity of the power supply systems with stochastic generation (due to renewable energy systems) are increasing. Ensuring secure operation of the system during widely varying loading scenarios or following possible unforeseen events represents an immense challenge to the system operator. Most of the recent methods of stability assessment are based on extensive off-line computations and, consequently, may no longer be sufficient; hence, a near-real-time DSA is significantly demanding. The near-real-time application of DSA to a realistic network needs sufficient methods to screen and rank large numbers of contingencies to be investigated by DSA tools.

In this paper, a transient stability-based fast and robust power system contingency screening and ranking method are proposed. Transient stability indices are generated from the AsDTM-based power system transient stability analysis results at each simulation time step. Two types of TS indices are evaluated. Those indices evaluated based on the analysis results of the machine's state variables (as rotor angle deviations (δ), angular speed ($\dot{\omega}$), etc) are represented as state variable indices (SI) and those evaluated based on the simulation results of the machine's bus complex bus voltages (such as bus voltage magnitude (V) and voltage angle (θ)) are represented as algebraic variable indices (AI). These indices are evaluated as the normalized weighted sum of squares of error at every simulation time step. As described in Section 3 above, compared with the classical DTM method the proposed AsDTM-based power system contingency screening and ranking method improves the accuracy of resulting indices by more than 74%. Similarly, compared with Rk4 and DTM the proposed AsDTM improves the total assessment time indices (evaluation + ranking) by more than 74.73% and 30.45%, respectively. This shows that the performance efficiency (performance speed) of the proposed method is significantly improved. The approach and indices are relatively simpler and can easily be integrated into an energy management system (EMS) or remedial action scheme (RAS) for determining the state of power system in case of large disturbances. Extending the approach for detail transient stability assessment of a near-real-time DSA session will be our next focus of research.

Author Contributions: Conceptualization, Methodology, software, formal analysis, investigation, resources, data curation, writing—original draft preparation, writing—review and editing, by T.L.K. Validation, visualization by T.L.K. and F.S. Supervision, project administration, by F.S. All authors have read and agreed to the published version of the manuscript.

Funding: This research received no external funding.

Data Availability Statement: All power flow data for the test cases are taken from the Matpower software package cited in the reference [29]. All dynamic data used for machines and their controllers are given in [24] Appendix A. Simulation codes are developed in a Matlab 2017b environment.

Conflicts of Interest: The authors declare no conflicts of interest.

References

1. Edwards, A.R. Detection of Instability in Power Systems Using Connectionism. Ph.D. Thesis, University of Bath, Bath, UK, 1995.
2. Tomsovic, K.L.; Sauer, P.W. *Vijay Vittal, Power System Stability and Control*; Taylor and Francis Group: London, UK, 2006.
3. Alvarez, J.M.G. Critical Contingencies Ranking for Dynamic Security Assessment Using Neural Networks. In Proceedings of the Intelligent System Applications to Power Systems, Curitiba, Brazil, 8–12 November 2009.
4. Tilman, J.; Weckesser, G. On-line Dynamic Security Assessment in Power Systems. Ph.D. Thesis, Department of Electrical Engineering Centre for Electric Power and Energy (CEE), Technical University of Denmark, Kongens Lyngby, Denmark, 2014.
5. Bose, A.; Fu, C. Contingency ranking based on severity indices in Dynamic Security Assessment. *IEEE Trans. Power Syst.* **1999**, *14*, 980–986.
6. Grillo, S.; Massucco, S.; Pitto, A.; Silvestro, F. Indices-based Voltage Stability Monitoring of the Italian HV Transmission System. In Proceedings of the Transmission & Distribution Conference and Exposition, New Orleans, LA, USA, 19–22 April 2010.
7. Kolluri, V.; Mandal, S.; Vaiman, M.Y.; Vaiman, M.M.; Lee, S.; Hirsch, P. Fast Fault Screening Approach to Assessing Transient Stability in Entergy's Power System. In Proceedings of the 2007 IEEE Power Engineering Society General Meeting, Tampa, FL, USA, 24–28 June 2007.
8. Oyekanmi, W.A.; Radman, G.; Ajewole, T.O. Transient stability based dynamic security assessment indices. *Cogent Eng.* **2017**, *4*, 1295506. [[CrossRef](#)]
9. Pai, M. *Energy Function Analysis for Power System Stability*; Kluwer Academic Publishers: London, UK, 1989.
10. Pavella, M.; Ernst, D.; Ruiz-Vega, D. *Transient Stability of Power Systems: A Unified Approach to Assessment and Control*; Kluwer Academic Publishers: London, UK, 2000.
11. Voropai, N.I.; Kurbatsky, V.G.; Tomin, N.V.; Panasetsky, D.A. Preventive and emergency control of intelligent power systems. In Proceedings of the 2012 IEEE PES Innovative Smart Grid Technologies (ISGT Europe), Berlin, Germany, 14–17 October 2012.
12. Fu, C.; Bose, A. Contingency Ranking Based on Severity Indices in Dynamic Security Analysis. *IEEE Trans. Power Syst.* **1999**, *14*, 980–985. [[CrossRef](#)]
13. Chadalavada, V.; Vittal, V.; Ejebe, G.C.; Irisarri, G.D.; Tong, J.; Pieper, G.; McMullen, M. An On-Line Contingency Filtering Scheme for Dynamic Security Assessment. *IEEE Trans. Power Syst.* **1997**, *12*, 153–161. [[CrossRef](#)]
14. Lee, B.; Kwon, S.H.; Lee, J.; Nam, H.K.; Choo, J.B.; Jeon, D.H. Fast contingency screening for online transient stability monitoring and assessment of the KEPCO system. *IEEE Proc. Gener. Transm. Distrib.* **2003**, *150*, 399–404. [[CrossRef](#)]
15. Xue, Y.; Pavella, M. Extended equal-area criterion: An analytical ultrafast method for transient stability assessment and preventive control of power systems. *Int. J. Electr. Power Energy Syst.* **1989**, *11*, 131–149. [[CrossRef](#)]
16. Xue, Y.; Huang, T.; Xue, F. Effective and Robust Case Screening for Transient Stability Assessment. In Proceedings of the 2013 IREP Symposium Bulk Power System Dynamics and Control—IX Optimization, Security and Control of the Emerging Power Grid, Rethymno, Greece, 25–30 August 2013; pp. 1–8.
17. Xue, Y.; Rousseaux, P.; Gao, Z.; Belhomme, R.; Euxible, E.; Heilbronn, B. Dynamic Extended Equal Area Criterion: Part 1. Basic formulation. In Proceedings of the IEEE/NTUA Athens Power Tech Conference, Athens, Greece, 5–8 September 1993; Volume 71, pp. 889–895.
18. Xue, Y.; Zhang, Y.; Gao, Z.; Rousseaux, P.; Wehenkel, L.; Pavella, M.; Trotignon, M.; Duchamp, A.; Heilbronn, B. Dynamic Extended Equal Area Criterion Part 2. Embedding fast valving and automatic voltage regulation. In Proceedings of the IEEE/NTUA Athens Power Tech Conference, Athens, Greece, 5–8 September 1993; Volume 71, pp. 896–900.
19. Liu, C.W.; Su, M.C.; Tsay, S.S.; Wang, Y.J. Application of a Novel Fuzzy Neural Network to Real-Time Transient Stability Swings Prediction Based on Synchronized Phasor Measurements. *IEEE Trans. Power Syst.* **1999**, *14*, 685–692.
20. Hashiesh, F.; Mostafa, H.E.; Khatib, A.R.; Helal, I.; Mansour, M.M. An intelligent wide area synchrophasor based system for predicting and mitigating transient instabilities. *IEEE Trans. Smart Grid* **2012**, *3*, 645–652. [[CrossRef](#)]
21. Liu, Y.; Sun, K. Solving Power System Differential Algebraic Equations Using Differential Transformation. *IEEE Trans. Power Syst.* **2019**, *35*, 2289–2299. [[CrossRef](#)]
22. El-Zahar, E.R. An Adaptive Step-Size Taylor Series Based Method and Application to Nonlinear Biochemical Reaction Model. *Trends. Appl. Sci. Res.* **2012**, *7*, 901–912.
23. El-Zahar, E.R. Applications of Adaptive Multi Step Differential Transform Method to Singular Perturbation Problems Arising in Science and Engineering. *Appl. Math. Inf. Sci.* **2015**, *9*, 223–232. [[CrossRef](#)]
24. Kumissa, T.L.; Shewarega, F. Fast Power System Transient Stability Simulation. *Energies* **2023**, *16*, 7157. [[CrossRef](#)]
25. Pukhov, E.; Georgii, G. Differential transformation method and circuit theory. *Int. J. Circuit Theory Appl.* **1982**, *10*, 265–276. [[CrossRef](#)]
26. Lindi, T.; Shewarega, F. Adaptive order and step-size differential transformation method-based power system transient stability simulation. *Aust. J. Electr. Electron. Eng.* **2024**, 1–14. [[CrossRef](#)]

-
27. Available online: <http://www.esat.kuleuven.be/electa/teaching/matdyn/> (accessed on 26 May 2020).
 28. The MathWorks Inc. *MATLAB (R2017b)*; The MathWorks Inc.: Natick, MA, USA, 2017.
 29. Zimmerman, R.D.; Murillo-Sánchez, C.E.; Thomas, R.J. MATPOWER: Steady-State Operations, Planning, and Analysis Tools for Power Systems Research and Education. *IEEE Trans. Power Syst.* **2011**, *26*, 12–19. [[CrossRef](#)]

Disclaimer/Publisher’s Note: The statements, opinions and data contained in all publications are solely those of the individual author(s) and contributor(s) and not of MDPI and/or the editor(s). MDPI and/or the editor(s) disclaim responsibility for any injury to people or property resulting from any ideas, methods, instructions or products referred to in the content.